


**Pseudospin polarization of composite fermions under uniaxial strain**Shuai Yuan<sup>1</sup>, Jiaojie Yan<sup>1,2</sup>, Ke Huang<sup>1,3</sup>, Zhimou Chen<sup>1</sup>, Haoran Fan<sup>1</sup>, L. N. Pfeiffer,<sup>4</sup>  
K. W. West,<sup>4</sup> Yang Liu,<sup>1,\*</sup> and Xi Lin<sup>1,5,6,†</sup><sup>1</sup>International Center for Quantum Materials, Peking University, Beijing 100871, China<sup>2</sup>Max Planck Institute for Solid State Research, Stuttgart 70569, Germany<sup>3</sup>Department of Physics, The Pennsylvania State University, University Park, Pennsylvania 16802, USA<sup>4</sup>Department of Electrical Engineering, Princeton University, Princeton, New Jersey 08544, USA<sup>5</sup>CAS Center for Excellence in Topological Quantum Computation, University of Chinese Academy of Sciences, Beijing 100190, China<sup>6</sup>Interdisciplinary Institute of Light-Element Quantum Materials and Research Center for Light-Element Advanced Materials, Peking University, Beijing 100871, China (Received 21 March 2023; revised 29 January 2024; accepted 2 February 2024; published 20 February 2024)

A two-dimensional system with extra degrees of freedom, such as spin and valley, is of great interest in the study of quantum phase transitions. The critical condition when a transition between different multicomponent fractional quantum Hall states appears is one of the very few junctions for many-body problems between theoretical calculations and experiments. In this work, we present that uniaxial strain induces pseudospin transitions of composite fermions in a two-dimensional hole gas. Determined from transport behavior, strain along  $\langle 111 \rangle$  effectively changes pseudospin energy levels. We deduce that diagonal strain dominates these variations. Our experiment provides a wedge for manipulating two-dimensional interacting systems mechanically.

DOI: [10.1103/PhysRevB.109.L081110](https://doi.org/10.1103/PhysRevB.109.L081110)

In two-dimensional systems at ultralow temperatures and high magnetic fields, exotic quantum states have been stabilized by the strong correlation between electrons. It is well known that noninteracting electrons form a series of discrete energy levels called Landau levels (LLs) in magnetic fields, and the filling factor  $\nu$  describes the number of occupied LLs. At different filling factors, two-dimensional electrons exhibit rich quantum phenomena, such as integer quantum Hall effect [1], fractional quantum Hall (FQH) effect [2], and charge density waves [3–8]. When a two-dimensional system has additional degrees of freedom, multicomponent quantum phases emerge. For example, at a particular filling factor, FQH states with different spin, valley, and subband compete with each other and transitions occur when those states become degenerate in energy. Such transitions can be induced by tuning the status of these components, such as tilted field [9–11], gate-tuning density [12,13], biaxial strain [14,15], and hydraulic pressure [16]. The energy separation between different possible states near the transition is universal, so its behavior can be compared with theoretical calculations, and provides an insight into a complex quantum system.

In general, holes in GaAs are subjected to strong spin-orbit interaction. The spin-orbit coupling in a two-dimensional system is affected by two kinds of asymmetry. One is bulk inversion asymmetry (BIA) which originates from the material's lattice structure and the other is structural inversion asymmetry (SIA) which depends on the effective out-of-plane electric field [17]. Uniaxial strain breaks the fourfold rotational symmetry and tunes the orbital motion of particles.

Previous investigations on FQH states under strain mostly focus on symmetry, such as reorientation of stripe phase [18] and anisotropy of Fermi contours [19–21]. However, the energy variation of FQH states under strain has been barely studied experimentally. The lowest two LLs share predominately  $N = 0$  character and are separated by an energy separation  $\Delta$  shown in Fig. 1(e). When  $\Delta$  is small, multicomponent FQH effects appear. Here, we report pseudospin polarization transitions at  $1 < \nu < 2$  induced by strain in a two-dimensional hole gas. Our result implies that the lattice deformation along  $\langle 111 \rangle$ ,  $\varepsilon_{\langle 111 \rangle}$ , tunes  $\Delta$  through the BIA and induces the observed transitions.

The GaAs/AlGaAs heterostructure sample in this work is grown on a GaAs (001) wafer by molecular beam epitaxy. Two-dimensional holes are confined to a 17.5-nm-wide symmetric GaAs quantum well, with carbon  $\delta$ -doped layers and undoped  $\text{Al}_{0.24}\text{Ga}_{0.76}\text{As}$  spacer layers on both sides. The carrier density is  $n_p \simeq 1.6 \times 10^{11} \text{ cm}^{-2}$ , and the mobility is larger than  $1 \times 10^6 \text{ cm}^2 \text{ V}^{-1} \text{ s}^{-1}$  at low temperatures. Our rectangular sample is dissociated along  $[110]$  and  $[\bar{1}\bar{1}0]$  which are denoted by  $X$  axis and  $Y$  axis. An L-shaped Hall bar is patterned in the  $1 \times 1 \text{ mm}^2$  center area of the sample, with ten InZn contacts around the edge of the pattern. We use epoxy to bond the sample, as shown on the inset of Fig. 1(a). The sandwich structure is mounted on a commercial uniaxial strain cell (Razorbill CS130) with homemade thermal connections and electrical filters. The strain cell applies uniaxial tension (pressure) on the sample and makes the sample expand (shrink) along the  $X$  axis, while the sample along the  $Y$  and  $Z$  axes is free and becomes shrunken (expanded). GaAs has a zinc-blende structure which consists of face centered cubic lattices of Ga and As atoms. The As lattices are a translation of Ga lattices in the diagonal direction  $\langle 111 \rangle$  of lattices. The

\*liuyang02@pku.edu.cn

†xilinf@pku.edu.cn

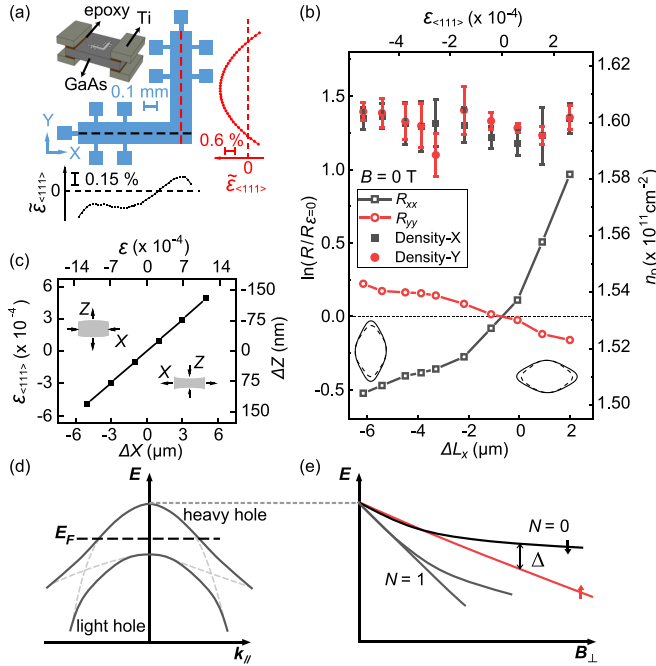


FIG. 1. Mechanical properties and transport properties of a GaAs sample. (a) Illustration of sample mounting, a pattern of an L-shaped bar, and strain distribution. Stress is applied along  $\langle 110 \rangle$ , paralleled with X axis. When the sample is compressed, the distribution of diagonal strain  $\bar{\epsilon}_{\langle 111 \rangle}$  along the black (red) dashed line is plotted nearby.  $\bar{\epsilon}_{\langle 111 \rangle}$  is defined as  $\epsilon_{\langle 111 \rangle} / \bar{\epsilon}_{\langle 111 \rangle} - 1$ . The diagonal strain  $\epsilon_{\langle 111 \rangle}$  is simulated through the software SOLIDWORKS, and  $\bar{\epsilon}_{\langle 111 \rangle}$  is the mean strain calculated from a  $1 \times 1 \text{ mm}^2$  area at the center of the sample. The configuration of the sample cell is shown as an inset. (b) Logarithm of longitudinal resistance  $R_{xx}$  ( $R_{yy}$ ) normalized by strain-free resistance  $R_{\epsilon=0}$ , and hole density  $n_p$ , as a function of displacement  $\Delta L_x$  at zero magnetic field. Traces of resistances cross at the zero-strain position. No apparent density shift is measured in our sample. Two small ellipses are diagrams of Fermi contour at positive and negative strain. The solid and dashed lines represent bands with different spins at  $k = 0$ . (c) Simulated mean diagonal strain, denoted by  $\bar{\epsilon}_{\langle 111 \rangle}$ , versus deformation displacement  $\Delta X$  when applying uniaxial strain along X axis. Simulated in-plane strain is defined as  $\epsilon = \epsilon_X - \epsilon_Y$ . When compressing with a reasonable value of  $5 \mu\text{m}$ , the sample is expected to have a significant  $\bar{\epsilon}_{\langle 111 \rangle}$  up to  $-4.9 \times 10^{-4}$ . The insets show exaggerated deformation of the sample in the X-Z plane. The difference between  $\Delta L_x$  in (b) and  $\Delta X$  in (c) suggests that the sample is subjected to a prepressurized status from the cooling down process. (d) Diagrams of valance bands in GaAs two-dimensional hole systems. Since the quantization along Z axis, the heavy-hole band and light-hole band show anticrossings and are mixed with each other [17]. (e) Landau level diagram of two-dimensional hole system. The nonlinear curves of Landau levels show strong spin-orbit coupling [17]. The arrows denote the pseudospins on the two lowest Landau levels.  $\Delta$  is the energy separation between the two lowest Landau levels.

strains along the X, Y, Z axes are projected to  $\langle 111 \rangle$  to form the strain along  $\langle 111 \rangle$ , namely diagonal strain  $\epsilon_{\langle 111 \rangle}$  [22]. We note that the diagonal strain on the sample has a linear dependence on the deformation displacement in Fig. 1(c). We use  $\bar{\epsilon}_{\langle 111 \rangle}$  to mark different strains applied on the sample in

this measurement. The simulated  $\epsilon_{\langle 111 \rangle}$  along the two arms is nearly uniform; see Fig. 1(a).

Uniaxial strain breaks the fourfold rotational symmetry of the Fermi contour, which becomes elongated along the direction where tensile strain is applied [19–21]. Therefore, the longitudinal resistances versus strain at zero magnetic field are plotted in Fig. 1(b). When tensing the sample along the X axis, the resistance of X arm increases rapidly as displacement  $\Delta L_x$  increases, while the resistance of the Y arm decreases. The phenomenon is consistent with anisotropic Fermi contours under strain [19–21]. When the resistances of two arms are the same at  $\Delta L_x = -0.68 \mu\text{m}$ , the transport is isotropic suggesting zero uniaxial strain. The small negative shift of displacement results from the thermal expansion of the piezo, even though the strain cell uses thermal-expansion-compensation technology [23].

The magnetoresistance traces of two arms at different  $\bar{\epsilon}_{\langle 111 \rangle}$  for  $1 < \nu < 2$  are shown in Fig. 2(a). All traces are measured at an effective temperature of about 41 mK using the same magnetic field ramping sequence. Transitions of FQH states around  $\nu = 3/2$  can be seen. Corresponding  $R_{xx}$  ( $R_{yy}$ ) minima of FQH states disappear and reappear with varying  $\bar{\epsilon}_{\langle 111 \rangle}$ . Note that the strength of the minima in the magnetoresistance traces is associated with the energy gaps of FQH states. Therefore, the energy gap undergoes a closing and reopening. The weakening positions of FQH states in Fig. 2(a) are marked by black diamonds. From the X-arm data, the  $5/3$  minimum becomes less clear when  $\bar{\epsilon}_{\langle 111 \rangle}$  declines to  $-5.4 \times 10^{-4}$ , and it tends to disappear if  $\bar{\epsilon}_{\langle 111 \rangle}$  further decreases. On the other side of  $\nu = 3/2$ , the  $4/3$  minimum is distinct at low strains, but becomes less clear when  $\bar{\epsilon}_{\langle 111 \rangle}$  declines, disappears at  $\bar{\epsilon}_{\langle 111 \rangle} = -3.7 \times 10^{-4}$ , and becomes distinct again at  $\bar{\epsilon}_{\langle 111 \rangle} = -5.4 \times 10^{-4}$ . Other FQH states exhibit the same behaviors as the  $4/3$  state. The  $8/5$ ,  $7/5$ ,  $11/7$ , and  $10/7$  minima disappear at  $\bar{\epsilon}_{\langle 111 \rangle} = -2.6 \times 10^{-4}$ ,  $-1.5 \times 10^{-4}$ ,  $-1.5 \times 10^{-4}$ , and  $-0.4 \times 10^{-4}$ , respectively. These behaviors measured in the Y arm are slightly quantitatively different from that measured in the X arm, due to the insignificant different value of strain distribution shown in Fig. 1(a). Other than that, traces of the Y arm are qualitatively similar to those of the X arm.

The transitions in Fig. 2(a) data can be explained by the pseudospin polarization transitions of composite fermions (CFs). CF is a quasiparticle consisting of one electron and even magnetic flux quanta. The interacting electrons in a magnetic field correspond to noninteracting CFs in an effective magnetic field [24]. Similar to LLs formed by electrons, CFs form a series of discrete energy levels called  $\Lambda$  levels and they are separated by CF's cyclotron energy  $\hbar\omega_{\text{CF}}$ . In Fig. 1(d), the GaAs quantum well confines holes along the Z axis and breaks the degeneracy of heavy-hole and light-hole bands. The two-dimensional holes occupy the doubly degenerate heavy-hole bands which consist of heavy heavy-hole (HHh) and light heavy-hole (LHh) subbands, see Fig. 1(d), and each subband generates a set of LLs. Within the axial approximation, the spin-orbit coupling mixes LLs with the same total angular momentum along the Z axis, resulting in a complicated LL diagram; see Fig. 1(e). In particular, the two lowest LLs have mostly  $N = 0$  characteristics and are separated by an energy  $\Delta$  determined by the spin-orbit coupling strength. We denote

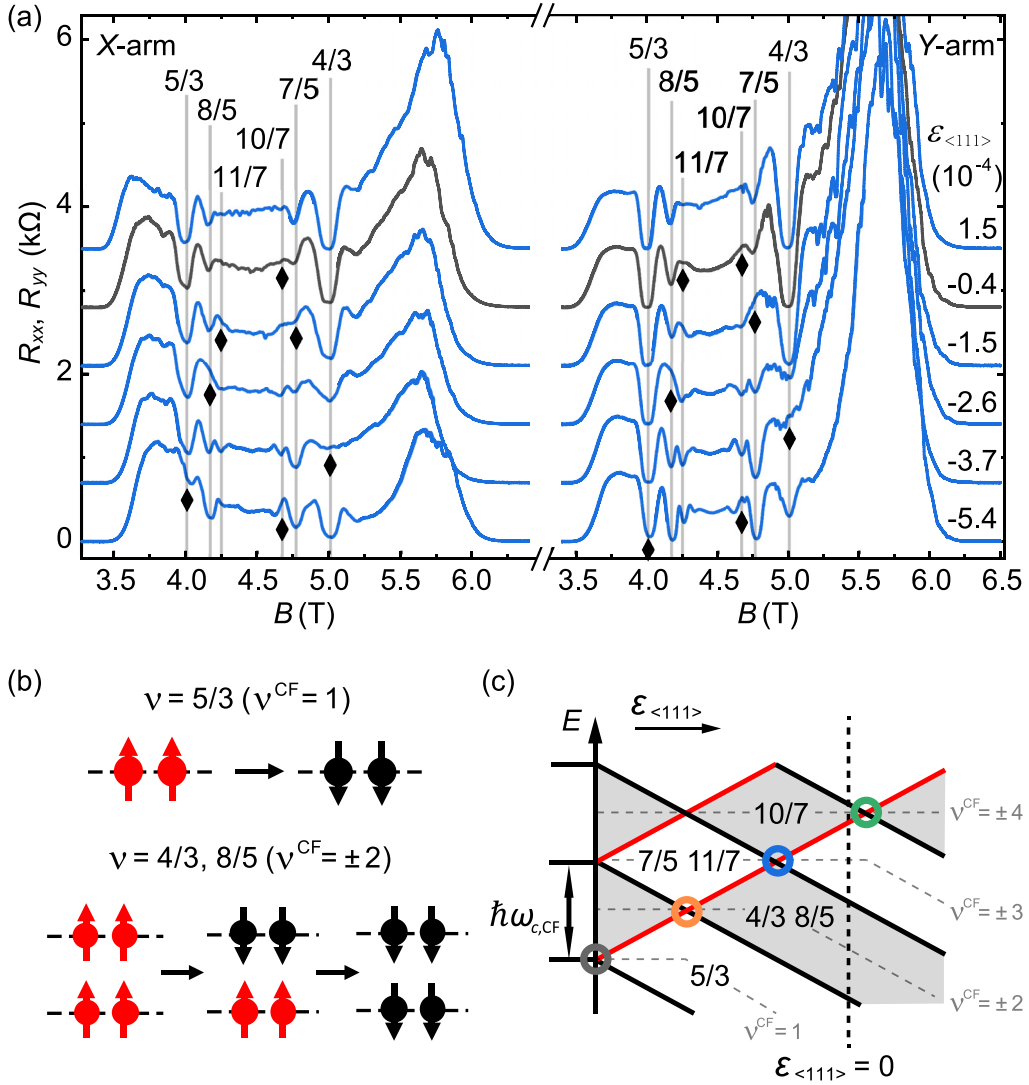


FIG. 2. (a) Longitudinal resistance traces of two arms measured under different strains at about 41 mK. Traces are offset vertically as multiples of  $700 \Omega$  for clarity. The values of applied diagonal strain  $\varepsilon_{\langle 111 \rangle}$  are shown on the right side of the Y-arm plot. The black trace shows data from the minimum strain. Possible FQH states are labeled by solid straight lines, based on the density calculated from Shubnikov-de Haas oscillations at low fields. Pseudospin transitions of FQH states take place at weakened minima of  $R_{xx}$  and are marked with black diamonds. (b) Cartoon charts of CFs with pseudospin degree of freedom. (c) Energy diagram of CF's  $\Lambda$  levels. Black and red solid lines represent  $\Lambda$  levels with down- or up-pseudospin, respectively. Strain  $\varepsilon_{\langle 111 \rangle}$  induces pseudospin splitting of  $\Lambda$  level and pseudospin transition at the crossing.

them by up-pseudospin ( $\uparrow$ ) and down-pseudospin ( $\downarrow$ ) respectively. When  $\Delta$  becomes comparable with  $\Lambda$  level separation, multicomponent FQH states with pseudospin degree of freedom form [17].

Compared with LLs, the relation between composite fermion  $\Lambda$  levels filling factor ( $\nu^{\text{CF}}$ ) and electron LLs filling factor ( $\nu$ ) is  $\nu = \nu^{\text{CF}} / (2\nu^{\text{CF}} + 1)$  when  $\nu < 1$ . Since the particle-hole symmetry,  $\nu$  equals  $2 - \nu^{\text{CF}} / (2\nu^{\text{CF}} + 1)$  when  $1 < \nu < 2$ . The CFs also retain a pseudospin degree of freedom, and each  $\Lambda$  level can be either up-pseudospin ( $\uparrow$ ) or down-pseudospin ( $\downarrow$ ). The  $\nu = 5/3$  ( $\nu^{\text{CF}} = 1$ ) state has only one  $\Lambda$  level, and can be either up-pseudospin ( $\uparrow$ ) or down-pseudospin ( $\downarrow$ ) fully polarized, as shown in Fig. 2(b). Similarly, the  $\nu = 4/3$  ( $\nu^{\text{CF}} = -2$ ) state has three different pseudospin ground states, ( $\uparrow\uparrow$ ), ( $\uparrow\downarrow$ ), and ( $\downarrow\downarrow$ ), and two pseudospin transitions.

In the CFs picture, the  $\nu = 5/3$  state has two pseudospin ground states. Unlike other FQH states, the ground states of  $\nu = 5/3$  are both fully polarized. The only transition between these two states, indicated by the increased longitudinal resistance, takes place when the energy separation of the pseudospin  $\Delta$  equals zero. The transition from an unpolarized  $\nu = 4/3$  state ( $\uparrow\downarrow$ ) to a fully polarized  $\nu = 4/3$  state ( $\uparrow\uparrow$  or  $\downarrow\downarrow$ ) is induced when the pseudospin energy separation  $\Delta$  is equal to the  $\Lambda$  level separation  $\hbar\omega_{\text{CF}}$ . Following the same rationale, we propose that  $\Delta$  increases as varying  $\varepsilon_{\langle 111 \rangle}$  so that the  $4/3$ ,  $8/5$ ,  $7/5$ ,  $10/7$ , and  $11/7$  states finally become fully polarized, illustrated as the energy diagram for CF  $\Lambda$  levels in Fig. 2(c). We summarize the  $R_{xx}$  normalized by resistance at  $\nu = 3/2$  in Fig. 3(a). The maxima marked by the arrows in Fig. 3(a) correspond to the last transitions marked by circles in Fig. 2(c), after which the FQH states become fully polarized.

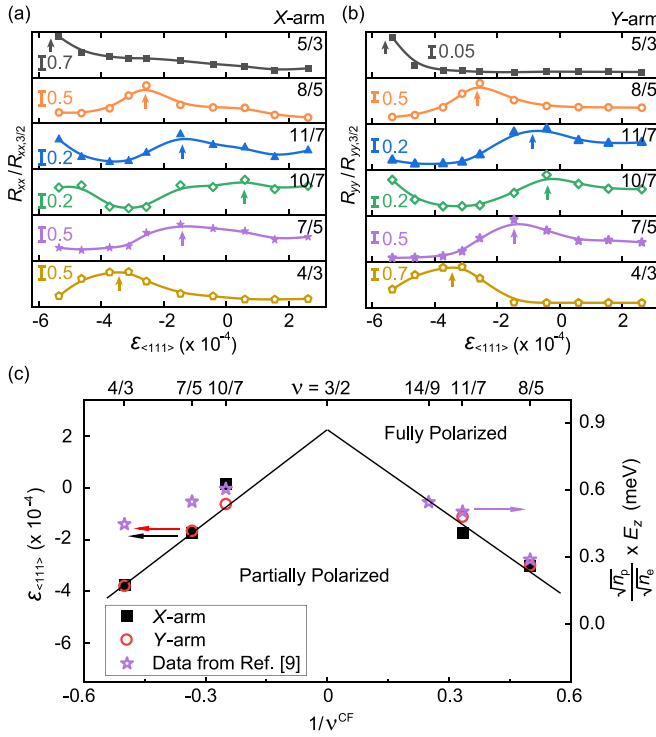


FIG. 3. (a), (b) Longitudinal resistance at different FQH states normalized to the nearly constant resistance of  $\nu = 3/2$  as a function of strain  $\varepsilon_{\langle 111 \rangle}$  along  $X$  arm and  $Y$  arm. The solid line in each trace is an eye guide for tendency. Arrows mark pseudospin transitions corresponding to circles in Fig. 2(c). (c) Phase diagram for the pseudospin polarization properties of CFs. The black square dots and red circular dots of the two arms are critical diagonal strains extracted from (a) and (b). The black solid lines drawn as an eye guide represent the phase boundary of the polarization transition. To compare data with spin transition in Ref. [9], the zero point of polarization energy is aligned with the minimum  $\varepsilon_{\langle 111 \rangle}$  where pseudospin energy separation  $\Delta \approx 0$ . Moreover, we assume that polarization energy in two different systems is the same order of magnitude, so the polarization energy is scaled by the ratio of Coulomb energy which is proportional to the square root of carrier density, since Coulomb energy  $V_c = e^2/(4\pi\epsilon l_B)$  and magnetic length  $l_B = \sqrt{\hbar/eB} = \sqrt{\nu/2\pi n}$ . The electron density in Ref. [9] is  $n_e = 1.13 \times 10^{11} \text{ cm}^{-2}$ , and the hole density in our sample is  $n_p = 1.61 \times 10^{11} \text{ cm}^{-2}$ .

From this figure,  $5/3$ ,  $4/3$ ,  $8/5$ ,  $7/5$ , and  $11/7$  states are fully polarized at zero strain [22].

For further analysis, we summarize the strain at the transitions to fully polarized states and plot a phase diagram in Fig. 3(c). The diagram shows that critical  $\varepsilon_{\langle 111 \rangle}$  needed to polarize FQH states decreases as  $|1/\nu^{\text{CF}}|$  increases, creating a “tent ( $\Delta$ )” shaped phase boundary. FQH states except the  $\nu = 5/3$  one are pseudospin-polarized above the tent, but pseudospin-partially polarized below the tent. Du *et al.* found a similar spin transition induced by an in-plane magnetic field in a GaAs two-dimensional electron gas with consistent conclusions [9]. The scaled polarization energy  $(\sqrt{n_p}/\sqrt{n_e})E_z$  represents the energy separation  $\Delta$  tuned by strain.

One might expect that  $\Delta$  variation might be related to the anisotropic Fermi contour, where positive and negative in-plane strain  $\varepsilon = \varepsilon_X - \varepsilon_Y$  correspond to anisotropy along

the  $X$  or  $Y$  axis, respectively. The GaAs (001) surfaces have a square symmetry, so the  $X$  axis is equivalent to the  $Y$  axis geometrically. As shown in Fig. 1(b), the resistance anisotropy  $|R_{xx} - R_{yy}|/|R_{xx} + R_{yy}|$  is an even function of the in-plane strain  $\varepsilon = \varepsilon_X - \varepsilon_Y$  which is proportional to  $\varepsilon_X$ . Thus, if  $\Delta$  were related to the anisotropy, one would expect it to be an even function of  $\varepsilon_X$ . However, the evolution in Figs. 3(a) and 3(b) and the phase diagram in Fig. 3(c) are clearly not evenly symmetric about  $\varepsilon_X$ . Therefore, the in-plane anisotropy is not likely the cause of variation in  $\Delta$ .

We suggest that the diagonal strain,  $\varepsilon_{\langle 111 \rangle}$  which monotonically depends on the displacement in Fig. 1(c), is likely the cause of the change of  $\Delta$ . In our nearly symmetric GaAs quantum well sample, the effective SIA is negligible. The BIA caused by the built-in dipole electric field along  $\langle 111 \rangle$  direction in GaAs dominates the spin-orbit coupling. The energy separation can be written as

$$\Delta = \frac{1}{2}(E_z - \hbar\omega_c) + \frac{1}{2}\sqrt{(\hbar\omega_c + E_z)^2 + 8\tilde{\eta}^2 \frac{eB}{\hbar}}, \quad (1)$$

where  $\omega_c$  is cyclotron angular frequency,  $E_z$  is Zeeman energy, and  $\tilde{\eta}$  is the prefactor related to BIA [17]. We estimate that the cyclotron energy  $\hbar\omega_c$  is about 1 meV and Zeeman energy  $E_z$  is about  $-0.5$  meV at  $\nu = 1 - 2$  in our sample.  $\Delta$  equals  $\sqrt{2\tilde{\eta}^2 eB/\hbar}$  at a small magnetic field, while it tends to  $E_z$  at a high magnetic field. Since the effective  $g$  factor of Zeeman energy is negative,  $E_z$  is negative, so  $\Delta = 0$  appears at some intermediate magnetic field; see Fig. 1(e). When we compress our sample along the  $X$  axis, the distance between Ga and As planes perpendicular to the  $\langle 111 \rangle$  direction decreases and the interatomic overlap increases. Our results suggest that the BIA-induced spin-orbit interaction  $|\tilde{\eta}|$  increases and the energy degenerate point ( $\Delta = 0$ ) moves to a higher magnetic field. The FQH states at  $\nu = 1 - 2$  are on the high-field side of the degenerate point [25]. These states tend to be pseudospin-unpolarized when spin-orbit interaction increases. In a previous study, hydrostatic pressure can also reduce the pseudospin separation of two-dimensional hole systems [16]. In Fig. 4, we compare the evolution of  $\nu = 5/3$  and  $4/3$  states induced by uniaxial strain and the hydrostatic pressure. The excitation gap of the  $\nu = 5/3$  state decreases, and that of the  $\nu = 4/3$  state decreases to zero and then increases whether the sample is compressed uniaxially or uniformly. A comparable feature is the weakening of the  $4/3$  state. It appears at 1.8 kbar in the hydrostatic pressure experiment, corresponding to critical  $\varepsilon_{\langle 111 \rangle} = -7.9 \times 10^{-4}$ , as well as at critical  $\varepsilon_{\langle 111 \rangle} = -3.6 \times 10^{-4}$  in our uniaxial strain experiments [22]. We note that hydrostatic pressure makes the sample shrink uniformly, while uniaxial compressive pressure makes the plane perpendicular to  $\langle 111 \rangle$  expand, which could be the result of the difference between the two experiments.

Examples with degrees of freedom controlled by strain are rare in two-dimensional systems. Electrons in the AIs quantum well occupy two in-plane conduction-band valleys at the  $X$  point in the Brillouin zone, and strain is well known to induce transitions through the valley [15,26]. GaAs systems do not share the valley degree of freedom, but here we find strain-induced pseudospin transitions. Compared with other methods for tuning degrees of freedom, strain avoids lots



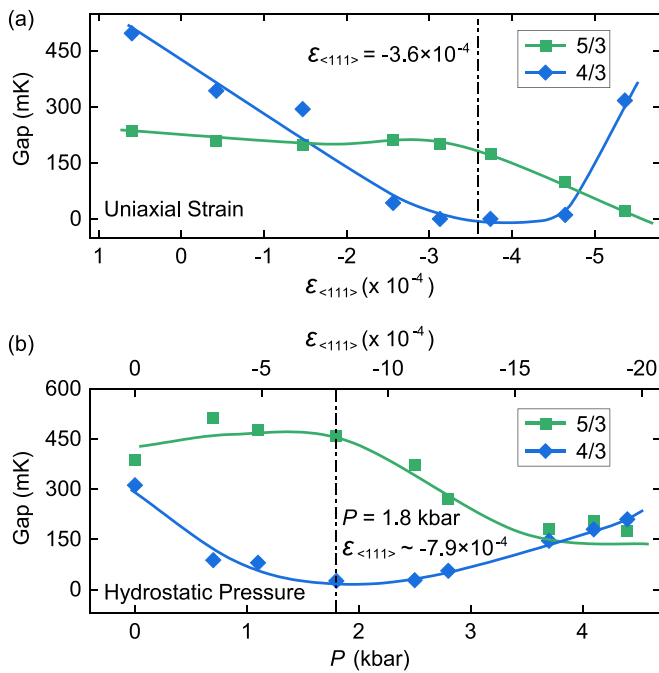


FIG. 4. Comparison of excitation gaps between uniaxial strain and hydrostatic pressure. (a) Excitation gaps of  $\nu = 5/3$  and  $4/3$  states under different uniaxial strains. The tendencies of traces are similar to those in hydrostatic pressure. (b) Data are from Ref. [16]. Since negative hydrostatic pressure, i.e., expanding samples uniformly, is hardly realized, the sample with hydrostatic pressure can only be compared with the compressed sample. The diagonal strains where the excitation gap of  $\nu = 4/3$  state is minimum are comparable in the two experiments.

of undesired effects. For example, the gate-tuning method varies both density and potential asymmetry together [12], and the tilted field method induces a finite-thickness effect to influence FQH states' stability [11]. Therefore, strain has the potential as a tool to probe multicomponent many-body states, such as non-Abelian even denominator states [27–30] and edge interactions between different polarization states [31].

In summary, we study the transport of two-dimensional hole gas systems confined in a symmetric quantum well. We observe the pseudospin transitions of CFs in a two-dimensional hole gas under strain, and propose that diagonal strain  $\varepsilon_{\langle 111 \rangle}$  rather than the in-plane strain plays a critical role in tuning the energy of different pseudospin bands. With the strain technique, precise mechanical control can be applied and we gain deeper insight into the complex energy structure of many-body states.

We thank P. Wang from Princeton University, and A. Ward and J. Barraclough from Razorbill Instruments Ltd for discussions. We acknowledge Prof. R. Winkler's help and permission to use the valance band sketch and Landau level diagram. The work at PKU was supported by the National Key Research and Development Program of China (Grant No. 2021YFA1401900), the NSFC (Grants No. 12141001 and No. 11921005), and the Strategic Priority Research Program of Chinese Academy of Sciences (Grant No. XDB28000000). The work at Princeton University was funded by the Gordon and Betty Moore Foundation through EPiQS Initiative Grant No. GBMF4420, by National Science Foundation MRSEC Grant No. DMR-1420541, and by the Keck Foundation.

- [1] K. v. Klitzing, G. Dorda, and M. Pepper, New method for high-accuracy determination of the fine-structure constant based on quantized Hall resistance, *Phys. Rev. Lett.* **45**, 494 (1980).
- [2] D. C. Tsui, H. L. Stormer, and A. C. Gossard, Two-dimensional magnetotransport in the extreme quantum limit, *Phys. Rev. Lett.* **48**, 1559 (1982).
- [3] V. J. Goldman, M. Santos, M. Shayegan, and J. E. Cunningham, Evidence for two-dimensional quantum Wigner crystal, *Phys. Rev. Lett.* **65**, 2189 (1990).
- [4] M. P. Lilly, K. B. Cooper, J. P. Eisenstein, L. N. Pfeiffer, and K. W. West, Evidence for an anisotropic state of two-dimensional electrons in high Landau levels, *Phys. Rev. Lett.* **82**, 394 (1999).
- [5] R. R. Du, D. C. Tsui, H. L. Stormer, L. N. Pfeiffer, K. W. Baldwin, and K. W. West, Strongly anisotropic transport in higher two-dimensional Landau levels, *Solid State Commun.* **109**, 389 (1999).
- [6] K. B. Cooper, M. P. Lilly, J. P. Eisenstein, L. N. Pfeiffer, and K. W. West, Insulating phases of two-dimensional electrons in high Landau levels: Observation of sharp thresholds to conduction, *Phys. Rev. B* **60**, R11285 (1999).
- [7] N. Deng, J. D. Watson, L. P. Rokhinson, M. J. Manfra, and G. A. Csáthy, Contrasting energy scales of reentrant integer quantum Hall states, *Phys. Rev. B* **86**, 201301(R) (2012).
- [8] D. Ro, S. A. Myers, N. Deng, J. D. Watson, M. J. Manfra, L. N. Pfeiffer, K. W. West, and G. A. Csáthy, Stability of multielectron bubbles in high Landau levels, *Phys. Rev. B* **102**, 115303 (2020).
- [9] R. R. Du, A. S. Yeh, H. L. Stormer, D. C. Tsui, L. N. Pfeiffer, and K. W. West, Fractional quantum Hall effect around  $\nu = 3/2$ : Composite fermions with a spin, *Phys. Rev. Lett.* **75**, 3926 (1995).
- [10] Y. Liu, S. Hasdemir, J. Shabani, M. Shayegan, L. N. Pfeiffer, K. W. West, and K. W. Baldwin, Multicomponent fractional quantum Hall states with subband and spin degrees of freedom, *Phys. Rev. B* **92**, 201101(R) (2015).
- [11] P. Wang, J. Sun, H. Fu, Y. Wu, H. Chen, L. N. Pfeiffer, K. W. West, X. C. Xie, and X. Lin, Finite-thickness effect and spin polarization of the even-denominator fractional quantum Hall states, *Phys. Rev. Res.* **2**, 022056(R) (2020).
- [12] K. Muraki and Y. Hirayama, Spin transition of a two-dimensional hole system in the fractional quantum Hall effect, *Phys. Rev. B* **59**, R2502(R) (1999).
- [13] Y. Liu, S. Hasdemir, A. Wójs, J. K. Jain, L. N. Pfeiffer, K. W. West, K. W. Baldwin, and M. Shayegan, Spin polarization of composite fermions and particle-hole symmetry breaking, *Phys. Rev. B* **90**, 085301 (2014).
- [14] O. Gunawan, Y. P. Shkolnikov, K. Vakili, T. Gokmen, E. P. De Poortere, and M. Shayegan, Valley susceptibility of an interacting two-dimensional electron system, *Phys. Rev. Lett.* **97**, 186404 (2006).

- [15] N. C. Bishop, M. Padmanabhan, K. Vakili, Y. P. Shkolnikov, E. P. De Poortere, and M. Shayegan, Valley polarization and susceptibility of composite fermions around a filling factor  $\nu = 3/2$ , *Phys. Rev. Lett.* **98**, 266404 (2007).
- [16] K. Huang, P. Wang, L. N. Pfeiffer, K. W. West, K. W. Baldwin, Y. Liu, and X. Lin, Resymmetrizing broken symmetry with hydraulic pressure, *Phys. Rev. Lett.* **123**, 206602 (2019).
- [17] R. Winkler, *Spin-orbit Coupling Effects in Two-Dimensional Electron and Hole Systems* (Springer, Berlin, 2003).
- [18] S. P. Koduvayur, Y. Lyanda-Geller, S. Khlebnikov, G. Csathy, M. J. Manfra, L. N. Pfeiffer, K. W. West, and L. P. Rokhinson, Effect of strain on stripe phases in the quantum Hall regime, *Phys. Rev. Lett.* **106**, 016804 (2011).
- [19] J. Shabani, M. Shayegan, and R. Winkler, Strain-induced fermi contour anisotropy of GaAs 2D holes, *Phys. Rev. Lett.* **100**, 096803 (2008).
- [20] I. Jo, M. A. Mueed, L. N. Pfeiffer, K. W. West, K. W. Baldwin, R. Winkler, M. Padmanabhan, and M. Shayegan, Tuning of Fermi contour anisotropy in GaAs (001) 2D holes via strain, *Appl. Phys. Lett.* **110**, 252103 (2017).
- [21] I. Jo, K. A. V. Rosales, M. A. Mueed, L. N. Pfeiffer, K. W. West, K. W. Baldwin, R. Winkler, M. Padmanabhan, and M. Shayegan, Transference of Fermi contour anisotropy to composite fermions, *Phys. Rev. Lett.* **119**, 016402 (2017).
- [22] See Supplemental Material at <http://link.aps.org/supplemental/10.1103/PhysRevB.109.L081110> for additional data and analysis, which includes Refs. [32–35].
- [23] C. W. Hicks, M. E. Barber, S. D. Edkins, D. O. Brodsky, and A. P. Mackenzie, Piezoelectric-based apparatus for strain tuning, *Rev. Sci. Instrum.* **85**, 065003 (2014).
- [24] J. K. Jain, *Composite Fermions* (Cambridge University Press, Cambridge, UK, 2007).
- [25] M. K. Ma, C. Wang, Y. J. Chung, L. N. Pfeiffer, K. W. West, K. W. Baldwin, R. Winkler, and M. Shayegan, Robust quantum Hall ferromagnetism near a gate-tuned  $\nu = 1$  Landau level crossing, *Phys. Rev. Lett.* **129**, 196801 (2022).
- [26] N. C. Bishop, M. Padmanabhan, O. Gunawan, T. Gokmen, E. P. De Poortere, Y. P. Shkolnikov, E. Tutuc, K. Vakili, and M. Shayegan, Valley susceptibility of interacting electrons and composite fermions, *Physica E* **40**, 986 (2008).
- [27] R. Willett, J. P. Eisenstein, H. L. Störmer, D. C. Tsui, A. C. Gossard, and J. H. English, Observation of an even-denominator quantum number in the fractional quantum Hall effect, *Phys. Rev. Lett.* **59**, 1776 (1987).
- [28] X. G. Wen, Non-Abelian statistics in the fractional quantum Hall states, *Phys. Rev. Lett.* **66**, 802 (1991).
- [29] X. Lin, R. Du, and X. Xie, Recent experimental progress of fractional quantum Hall effect: 5/2 filling state and graphene, *Nat. Sci. Rev.* **1**, 564 (2014).
- [30] K. K. W. Ma and D. E. Feldman, The sixteenfold way and the quantum Hall effect at half-integer filling factors, *Phys. Rev. B* **100**, 035302 (2019).
- [31] J. Liang, G. Simion, and Y. Lyanda-Geller, Parafermions, induced edge states, and domain walls in fractional quantum Hall effect spin transitions, *Phys. Rev. B* **100**, 075155 (2019).
- [32] S. Das Sarma and A. Pinczuk, *Perspectives in Quantum Hall Effects* (John Wiley & Sons, New York, 1997).
- [33] W. Young and R. Budynas, *Roark's Formulas for Stress and Strain* (McGraw-Hill, New York, 2002).
- [34] C. Wang, A. Gupta, Y. J. Chung, L. N. Pfeiffer, K. W. West, K. W. Baldwin, R. Winkler, and M. Shayegan, Highly anisotropic even-denominator fractional quantum Hall state in an orbitally coupled half-filled Landau level, *Phys. Rev. Lett.* **131**, 056302 (2023).
- [35] G. L. Bir and G. E. Pikus, *Symmetry and Strain-Induced Effects in Semiconductors* (Wiley, New York, 1974).